ELSEVIER

NeuroImage

www.elsevier.com/locate/ynimg
NeuroImage 35 (2007) 70–82

A multivariate analysis of neuroanatomic relationships in a genetically informative pediatric sample

J. Eric Schmitt,[a] Gregory L. Wallace,[b] Michael A. Rosenthal,[b] Elizabeth A. Molloy,[b] Sarah Ordaz,[b] Rhoshel Lenroot,[b] Liv S. Clasen,[b] Jonathan D. Blumenthal,[b] Kenneth S. Kendler,[a] Michael C. Neale,[a] and Jay N. Giedd[b,*]

[a]*Virginia Institute for Psychiatric and Behavioral Genetics and Departments of Psychiatry and Human Genetics, Virginia Commonwealth University, Richmond, VA 23298, USA*
[b]*Child Psychiatry Branch, National Institute of Mental Health, National Institutes of Health, Department of Health and Human Services, Bethesda, MD 20892, USA*

Received 7 December 2005; revised 21 March 2006; accepted 16 April 2006
Available online 5 January 2007

An important component of brain mapping is an understanding of the relationships between neuroanatomic structures, as well as the nature of shared causal factors. Prior twin studies have demonstrated that much of individual differences in human anatomy are caused by genetic differences, but information is limited on whether different structures share common genetic factors. We performed a multivariate statistical genetic analysis on volumetric MRI measures (cerebrum, cerebellum, lateral ventricles, corpus callosum, thalamus, and basal ganglia) from a pediatric sample of 326 twins and 158 singletons. Our results suggest that the great majority of variability in cerebrum, cerebellum, thalamus and basal ganglia is determined by a single genetic factor. Though most (75%) of the variability in corpus callosum was explained by additive genetic effects these were largely independent of other structures. We also observed relatively small but significant environmental effects common to multiple neuroanatomic regions, particularly between thalamus, basal ganglia, and lateral ventricles. These findings are concordant with prior volumetric twin studies and support radial models of brain evolution.

Introduction

The inception of neuroembryology might be considered to be when von Baer, over 175 years ago, first observed the neural tube in a vertebrate species and described its primordial subdivisions (von Baer, 1828). In the later half of the nineteenth century, Orr continued this work and detailed the initial segmentation of the nervous system into structural subunits, coined neuromeres, during embryogenesis in reptiles (Orr, 1887). Since these initial discoveries, neuroembryologists have chronicled the remarkable anatomical and cellular changes of the brain in great detail. Somehow, from the relative disorganization of the embryo evolves structure of extraordinary complexity. Despite its well-documented developmental sequence and our ever-expanding understanding of functional neuroanatomy, relatively little is known about the underlying forces responsible for the creation of the human brain. Presumably, our brain development is largely preordained by the genetic program given to us by our parents. Though heroic efforts in molecular genetics have identified thousands of genes with expression within the central nervous system (CNS) (Kandel and Jessl, 2000), attempts to explain normal human variation via genetic polymorphisms responsible for normal human variation in CNS structure have thus far had limited success.

The use of twin designs, wed with magnetic resonance imaging (MRI), provides a powerful non-invasive method to directly estimate the overall effects of genes and environment on human brain structure and function. Several previous studies have presented converging evidence that the predominant sources of variance in brain volumes are genetic in origin. Most studies performed to date have used small sample sizes (Bartley et al., 1997; Biondi et al., 1998; Steinmetz et al., 1995; Tramo et al., 1998), but a few more recent studies on larger samples have generally confirmed previous results (Baaré et al., 2001; Pennington et al., 2000). More recent twin designs also have included dizygotic twins, which enable the parsing of familial similarities into genetic and shared environmental sources. Though image processing methodologies differ substantially, univariate studies generally estimate that genes account for well over half of the variance in most volumetric regions of interest, particularly of the cerebral cortex. For example, Barré et al. reported that genes accounted for of 0.90, 0.82, and 0.88 of the total variance in total brain, gray, and white matter volumes, respectively, in 112 adult twin pairs (Baaré et al., 2001). Similarly, measures of the corpus callosum areas reveal heritabilities

* Corresponding author. National Institute of Mental Health, National Institutes of Health, Department of Health and Human Services, Room 4C110, 10 Center Dr. MSC 1367, Bethesda, MD 20892-1367, USA. Fax: +1 301 480 8898.
E-mail address: jg@nih.gov (J.N. Giedd).
Available online on ScienceDirect (www.sciencedirect.com).

1053-8119/$ - see front matter © 2006 Published by Elsevier Inc.
doi:10.1016/j.neuroimage.2006.04.232

of 0.80 or larger (Pfefferbaum et al., 2000, 2004; Scamvougeras et al., 2003). In contrast, there is virtually no evidence that environmental factors shared between twins influence cortical brain volumes (Pennington et al., 2000; Posthuma et al., 2000), although this may be obscured by non-additive effects of genes.

The sources of variability of noncortical structures are less well established, partially due to increased errors in measurement and partly because they are measured less often and usually in studies with quite small sample sizes. For example, the most comprehensive parcellation of the brain published in twins thus far was a study of 10 monozygotic (MZ) and 10 dizygotic (DZ) twin pairs (Wright et al., 2002). This study estimated heritabilities of 0.60 for corpus striatum, 0.79 for putamen, and 0.67 for the cerebellum, and 0.00 for the thalamus. These estimates, however, were not statistically different from zero owed to low statistical power. A study by White et al. found high interclass correlations in caudate, putamen, and thalamic volumes in a sample of 12 MZ twins compared to 12 control subjects (White et al., 2002). The role of genes in measures of ventricular volumes also has been uncertain. While the first examination of lateral ventricular volume in twins suggested high heritability (Reveley et al., 1984), subsequent investigations have found a more modest role of genes, if any (Baaré et al., 2001).

Though understanding the genetic epidemiology of individual brain regions is important in elucidating the biological substrates of neuroanatomic structure, determining how structures share common origins is equally vital. As yet, few imaging studies that have examined structural data in from a multivariate perspective, and with the exception of a handful of twin studies (Baaré et al., 2001; Pennington et al., 2000; Posthuma et al., 2000; SAS Institute, 2000; Wright et al., 2002), those have focused more on psychopathological disorders with putative disruptions in neural connectivity than on control populations (Faraone et al., 2003; Herbert et al., 2003; Tien et al., 1996; Wright et al., 1999). Such a dearth of information from in vivo structural studies is surprising given the great interest in functional connectivity and multivariate approaches in functional and diffusion tensor imaging (Ramnani et al., 2004). Determining typical patterns of anatomic relatedness, particularly in comparison to functional models, could be informative in disentangling the relative contributions of ontogenetic origin, subcranial environment, and functional connectivity in the development of neuroanatomic regions.

In this article, we attempt to fuse two lines of research, that of twin studies describing the genetic and environmental substrates of neuroanatomic endophenotypes with the rather limited literature examining the relationships between MRI volumetric measurements. Specifically, we employ factor analysis of several large brain structures (cerebrum, thalamus, lateral ventricles, telencephalic subcortical nuclei, corpus callosum, and cerebellum), of differing ontogenetic origins and diverse functions. Given our genetically informative sample, we also were able to investigate whether global factors exert their influence via genetic or non-genetic mechanisms.

Methods

Sample selection

127 pairs of monozygotic twins (mean age = 11.6, SD = 3.3; age range = 5.6–18.7; 74 [58%] male, 53 female) and 36 pairs of same-sex dizygotic twins (mean age = 11.0, SD = 3.7; age range = 5.5–18.2; 18 [60%] male, 12 female) were recruited by means of local and national advertisements for participation in an ongoing longitudinal pediatric brain MRI project at the Child Psychiatry Branch of the National Institute of Mental Health. The sample also included a group of 158 similarly recruited singletons (mean age = 11.3, SD = 3.5; age range = 5.2–18.7; 94 [59%] male, 64 female). Though singletons provide no genetic information, their addition substantially increased the precision of within-individual, cross-region correlations as well as total variance estimates for the phenotypes described below.

All subjects were screened via an initial telephone interview, parent and teacher rating versions of the Child Behavior Checklist (Achenbach and Ruffle, 2000), and physical and neurological assessment. Exclusion criteria included psychiatric diagnosis in the subject or a first-degree relative, and head injury or other conditions that might have affected gross brain development.

For twin recruitment, advertisements specified that the MRI study sought twins between the ages of 5 and 18, with no learning disabilities, neurological problems or behavioral disorders. The screening process involved phone interviews, behavioral questionnaires mailed to parents and teachers, an in-person clinical interview, family history assessment, as well as a physical and neurological exam. Exclusion criteria included having a lifetime history of physical, neurological, or psychiatric abnormalities, learning disabilities, or psychiatric illness oneself, or in either one first-degree relative or more than 20% of second-degree relatives. Approximately one in four families responding to the ads met inclusion criteria. Twins were included in the analysis only if quantifiable MRI scans free from motion or other artifact were obtained on both twins at the same age. Written assent from the child and written consent from a parent were obtained for each participant. The study protocol was approved by the institutional review board of the National Institute of Mental Health. Zygosity was determined by DNA analysis of buccal cheek swabs using 9–21 unlinked short tandem repeat loci for a minimum certainty of 99%, by BRT Laboratories, Inc. (Baltimore, MD).

Image acquisition

All subjects were scanned on the same GE 1.5 T Signa scanner using the same three-dimensional spoiled gradient recalled echo in the steady-state (3D SPGR) imaging protocol (axial slice thickness = 1.5 mm, time to echo = 5 ms, repetition time = 24 ms, flip angle = 45°, acquisition matrix = 192 × 256, number of excitations = 1, and field of view = 24 cm). A clinical neuroradiologist evaluated all scans and no gross abnormalities were reported.

Image processing

Images were analyzed using a previously described voxel-intensity-based classification of brain tissue into gray matter, white matter, or cerebrospinal fluid combined with a probabilistic atlas technique which informs which structure or region the voxel belongs to, based upon the voxel's location in standardized stereotactic space. Briefly, the raw MRI scans were first registered into standardized stereotaxic space using a linear transformation (Collins et al., 1994) and corrected for non-uniformity artifacts (Sled et al., 1998). The registered and corrected volumes were segmented into gray matter, white matter, cerebrospinal fluid, and background using a neural net classifier (Zijdenbos et al., 2002). The tissue classification information was combined with a probabilistic atlas to provide region of interest measures (Collins

et al., 1995). The output measures of this process that have shown high agreement with conventional hand tracing measures, and were included in this analysis, are the midsagittal area of the corpus callosum, the gray and white matter volumes of the total cerebrum, the caudate nucleus, the cerebellum, and the lateral ventricles.

The resultant regions of interest obtained from image segmentation were gray and white lobar volumes, cerebellum, thalamus, lateral ventricles, globus pallidus, putamen, caudate nucleus, and corpus callosum. To make the experiment more computationally manageable, we chose 6 gross regions of interest that represent different ontogenetic origins and neurological functions. Namely, we measured total cerebral volume (sum of gray plus white lobar volumes), the midsagittal area of the corpus callosum (CC), lateral ventricles (LV), thalamic nuclei, basal ganglia (sum of caudate nucleus, globus pallidus, and putamen; BG), and the total cerebellar volume.

Statistical analyses

Since our structural models assume normally distributed variables, prior to analyses the distributions of all variables were inspected for normality. All volumes appeared to be normally distributed, with the exception of lateral ventricles which had a leftward skew, caused by several outliers above the bulk of the distribution. Using SAS, we calculated descriptive statistics for all regions of interest (SAS Institute, 2000). We also calculated correlations between all volumes for visual inspection prior to modeling. Since preliminary simple linear regressions demonstrated a significant effect of age, race, and sex, we used residuals from multiple regressions including age sex and race as explanatory variables. Thus, the resultant partial correlation matrix represents inter-anatomic relationships after removing the effects of age, sex, and race.

Raw data were imported into Mx (Neale et al., 1999) for multivariate genetic analyses. Multivariate approaches enable the detection of common factors that influence multiple regions similarly, or alternatively can demonstrate independence of one structure relative to another. The multivariate approach also substantially increases power, as the use of inter-structure correlations provides additional information which improves statistical precision (Schmitz et al., 1998). The presence of genetically informative data additionally allows the parsing of total variance of each structure into contributions from additive genetic (A), shared environmental (C) and unique environmental components (E) based on the differences in genetic correlations between MZ and DZ twins (Neale and Cardon, 1992).

We attempted to model the relationships between structures via two alternative techniques. In addition to traditional factor analytic approaches (described below), we also constructed Cholesky decompositions to calculate descriptive statistics of broad sense heritability and genetic correlations. In all models, we employed maximum likelihood (Edwards, 1972) in order to generate the most probable parameter estimates (i.e., maximum likelihood estimates) for any given model. All models also included a means component that regressed out the contributions of sex, age, and race to the variance in each neuroanatomic region of interest (ROI).

Cholesky decompositions

We used Cholesky factorization to calculate genetic and environmental correlation matrices, as well as estimates of the proportion of variance due to genetic (a^2), shared environment (c^2), and unique environment (e^2). This procedure deconstructs any $n \times n$-positive definite variance–covariance matrix into an $n \times n$ triangular matrix postmultiplied by its transpose (Neale and Cardon, 1992), and places few a priori constraints on the fitting of the data. Since the parameters of a Cholesky decomposition imply directionality of the latent factors, their direct interpretation is probably inappropriate for the present data (Loehlin, 1996). However, the approach permits unbiased estimation of inter-structure correlations, parceled into relationships of either genetic or environmental origin (Crawford and DeFries, 1978). The genetic correlation, which measures the degree of overlap between the genetic forces on two phenotypes, can be written mathematically as:

$$r_{x,y} = \frac{A_{xy}}{\sqrt{(A_x * A_y)}}$$

where A_{xy} is the genetic covariance between structures x and y, and A_x and A_y represent the proportion of the variance due to genetic factors for x and y, respectively (Falconer and Mackay, 1996). Similar calculations can be used to measure the role of shared and unique environment. We also determined the proportion of genetic, shared environmental, and unique environmental covariance relative to the total phenotypic variance. Finally, we calculated eigenvalues from standardized covariance matrices (i.e., correlation matrixes) for these analyses for A, C, and E separately, to estimate the best number of latent factors to employ in subsequent analyses.

Factor analyses

A common goal of multivariate analysis is to extract latent constructs that explain the covariance between observed measures. Ideally, the relationship between a large set of variables can be accounted for by a relatively small number of factors. In our analyses, we tested two families of models; that of the independent pathway (i.e., biometric) and the common pathway (i.e., psychometric) models (Kendler et al., 1987; Mcardle and Goldsmith, 1990; Neale and Cardon, 1992). Independent pathways models (IPM) allow genetic, shared environmental, and unique environmental common factors to affect observed variables directly, while in common pathways models (CPM) these factors exert their influence through a shared, latent phenotype (Fig. 1). In both models, each observed variable is permitted a residual variance term, which can also be parsed into A, C, and E (Evans et al., 2002). Though IPMs are conceptually simpler, CPMs require fewer parameters and are thus favored by the rules of parsimony, all things being equal. However, in the case of neuroanatomic data, a biometric structure would seem the superior hypothesis, as genetic and environmental factors would be expected to impact brain volumes directly via independent channels.

In addition to models with a single common factor for each of the three etiological sources (A, C, and E), we also constructed more complex models which allowed for 2 common factors for each variance component (Fig. 2); two-factor solutions were suggested by a scree plot of eigenvalues from the Cholesky decomposition. The models are near the upper limit of mathematical feasibility (i.e., they are close to being underidentified) for a six-variable multivariate analysis. We designated the most complex of these the 2-2-2 IPM and 2-2-2 CPM models since they each contain 2 additive genetic, 2 shared environmental, and 2 unique

environmental common factors. For models with 2 common factors of identical etiology (i.e., genetic), we arbitrarily removed one path from the second factor to an observed variable (cerebrum) in order to fix the rotational indeterminacy inherent in models with two or more factors.

Under certain regularity conditions, the difference in −2 times the log likelihood (−2LL) of any model and a nested submodel follows a χ^2 distribution with degrees of freedom equal to the difference in the number of parameters. Therefore, we could directly test whether simpler models fit the data significantly worse than more complex versions. In particular, we were interested in determining whether shared environmental factors are important in explaining covariance, since prior univariate analyses would suggest that the shared environment has little to no impact on the variability of most brain regions. For all comparisons, we also calculated Akaike's information criteria (AIC), as χ^2-2*df, which rewards parsimony in addition to goodness of fit (Akaike, 1987); negative values imply that the nested submodel is a more parsimonious fit than the full comparison model.

From the best-fit model (2-0-2 IPM), we standardized parameter estimates to facilitate interpretation and performed orthogonal rotation via the VARIMAX procedure in SAS (SAS Institute, 2000). In order to generate likelihood-based confidence intervals on the rotated parameter estimates (Neale and Miller, 1997), we reran the best-fit model in Mx, but freed the two paths previously fixed to zero and instead fixed the rotated factor loadings of the 2nd A and E common factors that were closest to zero. As an alternative and perhaps more familiar metric of the statistical significance of individual parameters, we also attempted to drop each parameter from the model and test whether the fit to the data deteriorated significantly. This approach is therefore completely analogous to tests of significance of individual beta weights in a multiple regression model.

Gray/white cerebral comparisons

Our primary analyses combined cerebral gray and white matter volumes into a single variable, since we had no tissue-specific information for non-cerebral structures. However, since other studies have analyzed gray/white differences (Baaré et al., 2001), we calculated genetic and environmental correlations from a Cholesky decomposition that split total cerebral volume into gray and white matter in order to facilitate comparisons between studies.

Covarying for total brain volume

To investigate *relative* differences in inter-structure covariance rather than *absolute* differences, we repeated the factor analysis procedure described above, but included total brain volume (TBV) as a regressor and repeated the analyses. With the exception of

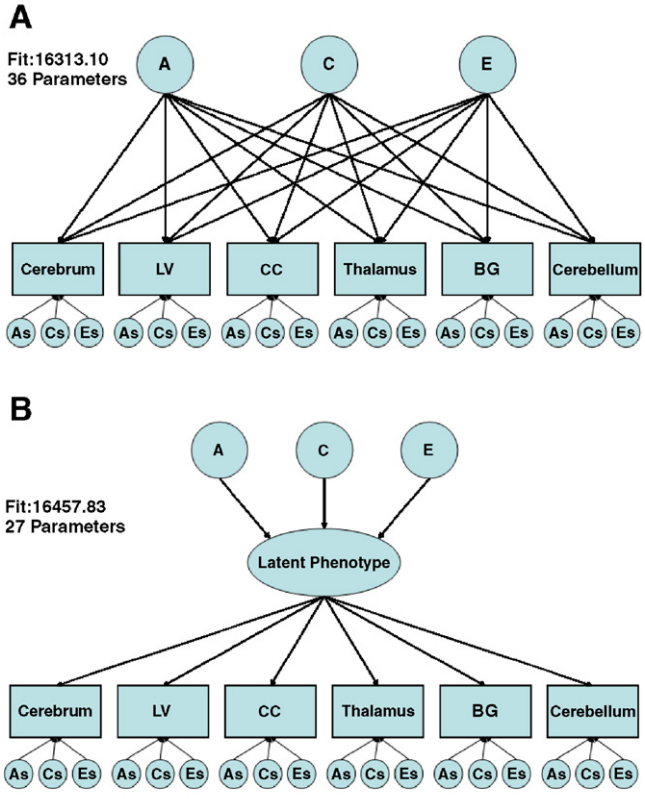

Fig. 1. Two putative factor models for explaining covariance in neuroanatomic data. While the independent pathways model (A) allow genes A, C, and E to directly influence the observed variables, the common pathways model (B) their effects are mediated via a shared latent variable. A, C, and E are modeled to have means of zero and variances of one. For both models, residual variance can be partitioned as well; thus if common factors are removed, both models collapse to univariate analyses run in parallel.

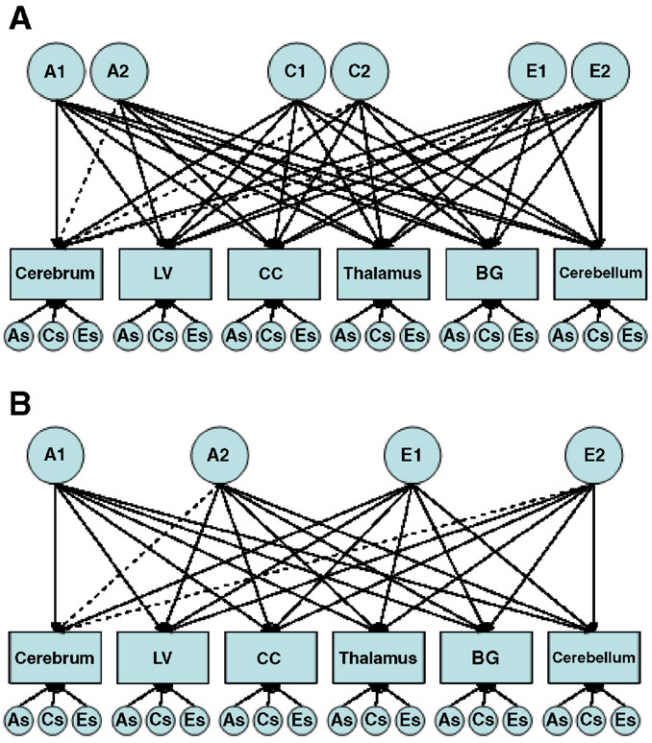

Fig. 2. Examples of expanded models allowing for multiple factors for each variance component. The 2-2-2 IPM (A) represented the most complex model that was fit to the data; all other models were nested submodels of the 2-2-2 IPM. Dotted lines represent parameters that were fixed to zero in order to make factors orthogonal. The 2-0-2 IPM (B) represents the best-fit model, both by χ^2 tests and AIC.

adjusting for TBV, our mathematical modeling approach was identical to that described previously.

Results

Descriptive statistics

Means and standard deviations for all measures are given in Table 1. Singletons, MZs, and DZs had comparable means and variances for all structures measured. A cross-twin correlation matrix for both MZ and DZ groups is provided in Table 2. In general, within-structure, cross-twin correlations were substantially higher in the MZ than in the DZ twins, suggesting a strong role of genetic factors on the variance in brain volumes. The role of genetic factors in the cerebellum appeared to be more modest, and even less prominent for the lateral ventricles. When examining within-individual, cross-structure correlations the cerebrum, thalamus, and basal ganglia were highly intercorrelated. Correlations with the lateral ventricles were low; indeed a small negative correlation was observed between the basal ganglia and lateral ventricular volumes. The corpus callosum also was not correlated with other structures. The cross-twin, cross-structure correlations are much greater in MZ than DZ twins, suggesting that much of the observed correlations between structures are genetically mediated.

Variance components estimates from the Cholesky decomposition are given in Fig. 3. As expected, neural tissue demonstrated high heritability, with the cerebellum slightly lower than other structures. The variance in lateral ventricular volume was equally divided between genetic, shared environmental and unique environmental sources. Table 3 reports genetic and environmental correlations and reveals the extent to which different structures share genetic and environmental sources of variance. The genetic substrates of cerebrum, thalamus, basal ganglia, and cerebellum are highly intercorrelated. There was a small but statistically significant genetic correlation between corpus callosum and cerebrum, thalamus, and basal ganglia. Cross-structure correlations attributable to the unique (i.e., individual-specific) environment were generally lower, but were still substantial between thalamus and basal ganglia and between cerebrum and cerebellum. Interestingly, there was a small but statistically significant negative environmental correlation between the lateral ventricles and both thalamus and basal ganglia.

Table 1
Descriptive statistics for all anatomic structures analyzed in the present study, split by zygosity status

	MZ (N=180)		DZ (N=72)		Singletons (N=158)	
	Mean	SD	Mean	SD	Mean	SD
Total cerebrum	1104.59	107.03	1111.63	100.62	1106.06	111.72
Lateral ventricles	11.71	6.13	10.80	5.21	10.90	6.01
Corpus callosum	529.99	69.48	527.50	62.32	530.83	81.53
Thalamus	17.22	1.35	17.21	1.38	17.50	1.55
Basal ganglia	25.04	2.17	25.47	2.17	25.67	2.41
Cerebellum	131.43	11.79	129.84	12.06	129.83	12.26
Cerebral gray matter	725.07	68.09	730.88	60.66	726.05	75.14
Cerebral white matter	379.52	49.79	380.75	48.09	380.01	51.18

Mid-sagittal corpus callosum is measured in square millimeters, while the volumetric measures are in cubic centimeters.

Table 2
Cross twin correlation matrix of six neuroanatomic regions

	Cer1	LV1	CC1	Thal1	BG1	Cb1	Cer2	LV2	CC2	Thal2	BG2	Cb2
Cer1	**1.00**	**0.22**	**0.29**	**0.75**	**0.77**	**0.68**	**0.34**	**0.08**	**−0.37**	**0.37**	**0.42**	**0.38**
LV1	0.34	**1.00**	**−0.09**	**0.06**	**−0.05**	**0.27**	**0.19**	**0.39**	**−0.08**	**0.11**	**0.15**	**0.10**
CC1	0.15	0.02	**1.00**	**0.31**	**0.15**	**0.22**	**0.18**	**−0.08**	**0.26**	**0.18**	**0.14**	**0.22**
Thal1	0.80	−0.06	0.15	**1.00**	**0.90**	**0.50**	**0.20**	**0.04**	**−0.41**	**0.32**	**0.34**	**0.42**
BG1	0.76	−0.11	0.27	0.91	**1.00**	**0.53**	**0.26**	**0.07**	**−0.46**	**0.27**	**0.33**	**0.41**
Cb1	0.58	0.26	0.23	0.48	0.43	**1.00**	**0.13**	**0.09**	**−0.10**	**0.13**	**0.22**	**0.54**
Cer2	**0.88**	0.10	0.17	0.66	0.69	0.57	**1.00**	**0.12**	**0.28**	**0.77**	**0.85**	**0.67**
LV2	0.14	**0.65**	−0.01	−0.05	−0.15	0.15	0.28	**1.00**	**−0.16**	**−0.03**	**−0.05**	**0.15**
CC2	0.29	0.09	**0.83**	0.24	0.17	0.23	0.09	0.04	**1.00**	**0.30**	**0.19**	**0.23**
Thal2	0.75	0.03	0.19	**0.80**	0.79	0.51	0.86	−0.09	0.22	**1.00**	**0.96**	**0.56**
BG2	0.76	0.00	0.21	0.75	**0.83**	0.52	0.78	−0.16	0.27	0.94	**1.00**	**0.56**
Cb2	0.59	0.09	0.18	0.52	0.53	**0.79**	0.69	0.30	−0.01	0.63	0.63	**1.00**

MZ correlations are shown below the diagonal, while DZ twins are above. Within-structure, cross-twin correlations are shown in bold. Abbreviations are as follows: Cer—cerebrum, LV—lateral ventricles, CC—corpus callosum, Thal—thalamus, BG—basal ganglia, Cb—cerebellum.

The role of the environment, however, was quite minor relative to the impact of genetic structures on neuroanatomic covariance. Since the environmental correlation represents the proportion of unique *environmental* variance shared between two structures, it excludes variance attributable to other sources. In other words, these values are standardized relative to the unique environmental variance components, which can be quite small. Table 4 reports how genetic and environmental covariance relates to the *total* phenotypic variance in each structure. The highest shared environmental correlation was 0.17, and the highest unique environmental correlation was 0.12, with most values near zero. In contrast, the majority of the genetic correlations were greater than 0.20, with the highest (basal ganglia versus thalamus) estimated at 0.70.

Factor analyses

Our most parameterized model, the 2-2-2 IPM, did not fit the data significantly worse than the fully saturated Cholesky, despite its comparative simplicity (χ^2_{12}=10.2, p=0.5980, AIC=−13.8). The 2-2-2 CPM also did not differ significantly from the full Cholesky (χ^2_{27}=35.08, p=0.1369, AIC=−18.92) but was more parsimonious. The relative equivalence between the IPM and CPM models was driven by the eleven shared environmental common parameters in the IPM that were largely uninformative. Removing these parameters (producing the 2-0-2 IPM) did not significantly affect the fit of the model (versus full Cholesky: χ^2_{23}=17.0, p=0.8093, AIC=−29.0; versus 2-2-2 IPM: χ^2_{11}=6.8, p=0.8147, AIC=−15.2) and produced superior explanation of the data compared to the 2-2-2 CPM. Further attempts at reduction of the 2-0-2 IPM were unsuccessful (versus 1-0-2 IPM: χ^2_5=20.4, p=0.0011, AIC=10.4; versus 2-0-1 IPM: χ^2_5=61.8; p<0.0001; AIC=51.8), as were other factorial combinations of IPM and CPM submodels.

The varimax-rotated parameter estimates for the 2-0-2 IPM are given in Table 5. Of the two common genetic factors identified, one strongly influenced variance of cerebrum, thalamus, and basal ganglia, with factor loadings (analogous to standardized partial regression coefficients) of about 0.85. This factor also accounted for a substantial proportion of the genetic variance of the cerebellum, and had a low but statistically significant effect on corpus callosum, but no impact on lateral ventricular volumes. The second genetic factor predominantly comprised the modest genetic effects on ventricular volume, with a statistically significant negative factor loading on the basal ganglia compartment.

Similarly, two unique environmental common factors were identified, though the pattern of effects was quite different than that of the genetic factors. One environmental factor primarily contributed to variance in all deep structures (thalamus, BG, LV, and corpus callosum), with antagonism between the ventricles and the other variables. The second represented relationships between the cerebrum, lateral ventricles, and cerebellum.

Structure-specific factors contributed far less variance than the common factors with the exception of the corpus callosum where genetic factors specific to that structure accounted for 69% of the variance. Less than 10% of the variance in corpus callosum size could be explained by genetic sources that also affected other structures in the analysis.

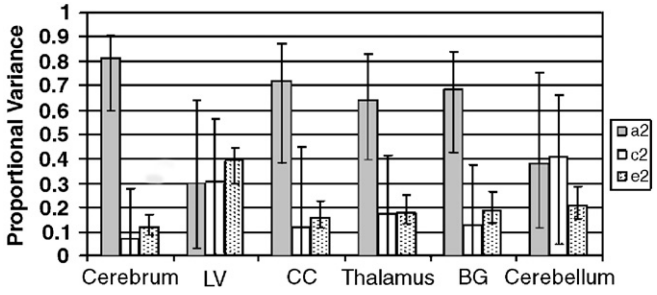

Fig. 3. Variance components estimates obtained from Cholesky decomposition. a^2, c^2, and e^2 represent the proportion of variance due to additive genetic, the shared environment, and the unique environment, respectively. Bars denote likelihood-based 95% confidence intervals.

Table 3
Sources of correlation between neuroanatomic regions

	Cerebrum	LV	CC	Thalamus	BG	Cerebellum
Cerebrum	1	**0.26 (0.06 0.43)**	**0.37 (0.17 0.54)**	**0.35 (0.16 0.51)**	**0.23 (0.03 0.42)**	**0.58 (0.43 0.70)**
LV	0.18 (−0.33 0.69)	1	**−0.05 (−0.25 0.15)**	**−0.22 (−0.40 −0.03)**	**−0.23 (−0.41 −0.03)**	**0.29 (0.10 0.46)**
CC	0.30 (0.05 0.52)	0.22 (−0.54 0.74)	1	**0.49 (32 0.63)**	**0.39 (0.19 0.55)**	**0.10 (−0.11 0.30)**
Thalamus	0.97 (0.83 1.0)	0.00 (−0.49 0.65)	0.42 (0.11 0.66)	1	**0.65 (0.52 0.75)**	**0.07 (−0.13 0.27)**
BG	0.82 (0.71 0.92)	−0.37 (−0.80 0.24)	0.35 (0.07 0.64)	0.91 (0.81 0.98)	1	**0.13 (−0.07 0.33)**
Cerebellum	0.82 (0.59 1.0)	0.20 (−0.59 0.71)	0.12 (−0.38 0.57)	0.79 (0.44 1.0)	0.63 (0.29 0.93)	1

Genetic correlations are given below the diagonal; unique environmental correlations are above it. 95% confidence intervals are given in parenthesis. Estimates of shared environmental correlations all had extremely wide confidence intervals and were uninformative; therefore they are not reported.

Gray/white correlations

Genetic correlations between cerebral tissue compartments and other structures are given in Table 6. The genetic effects influencing gray and white were highly correlated (0.84; 95% CI [0.65 0.99]), while there was virtually no environmental correlation (−0.04; 95% CI [−0.24 0.17]). In general, correlations did not differ when comparing either cerebral gray or white to other structures. The primary exception was corpus callosum, which had higher genetic (0.49 versus 0.09) and environmental (0.43 versus 0.16) correlations with cerebral white matter volumes relative to gray. Additionally, the environmental correlation between cerebellum and cerebral gray (0.57) was significantly higher than cerebellum with cerebral white (0.22).

Total brain volume as a covariate

As expected from the previous finding that a single genetic factor dominated inter-structure covariance, the genetic correlations between structures dropped substantially when adjusting for total brain volume (Table 7). We still detected a high, statistically significant genetic correlation between thalamus and basal ganglia (r_G=0.72), and a negative genetic correlation between basal ganglia and the lateral ventricles (r_G=−0.88). The non-genetic inter-structure correlations, however, differed substantially when the analyses were adjusted for global effects. Rather than a general pattern of positive correlations between structures detected previously (with the exception of negative correlations involving lateral ventricles), the environmental correlations had a more complex pattern. Both the thalamus and basal ganglia structures were *negatively* correlated with cerebral volumes, but positively correlated with each other. The lateral ventricles retained their mostly negative environmental correlations with other structures. There was a small but statistically significant negative environmental correlation between the cerebellum and the thalamus, and all telencephalic tissues showed negative correlations with the cerebellum, though none approached statistical significance.

When performing factor analyses after covarying for TBV, the 2-2-2 IPM (χ^2_{i2}=8.1; p=0.7807; AIC=−15.94) did not fit the data

Table 4
Variance components relative to the total phenotypic variance, with 95% confidence intervals provided

	Cerebrum	LV	CC	Thalamus	BG	Cerebellum
Cerebrum	**0.12 (0.09 0.17)** ***0.05 (0.00 0.29)*** **0.82 (0.59 91)**	0.06 (0.01 0.11) *0.08 (−0.12 0.27)*	0.05 (0.02 0.09) *0.01 (−0.13 0.20)*	0.05 (0.02 0.09) *0.02 (−0.06 0.23)*	0.03 (0.00 0.07) *0.07 (−0.03 0.28)*	0.09 (0.06 0.14) *0.13 (−0.05 0.37)*
LV	0.09 (−0.12. 23)	**0.40 (0.29 0.53)** ***0.30 (0.00 0.57)*** **0.31 (0.03 0.64)**	−0.01(−0.07 0.04) *−0.08 (−0.27 0.19)*	−0.06 (−0.12 −0.01) *0.04 (−0.17 0.23)*	−0.06 (−0.13 −0.01) *0.12 (−0.11 0.27)*	0.08 (0.03 0.15) *0.07 (−0.20 0.33)*
CC	0.23 (0.03 0.39)	0.10 (−0.18 0.31)	**0.16 (0.11 0.23)** ***0.13 (0.00 0.46)*** **0.71 (0.38 0.87)**	0.08 (0.05 0.13) *−0.01 (−0.16 0.21)*	0.07 (0.03 0.12) *−0.03 (−0.18 0.17)*	0.02 (−0.02 0.06) *0.10 (−0.15 0.33)*
Thalamus	0.70 (0.50 0.80)	0.00 (−0.20 0.22)	0.29 (0.06 0.45)	**0.18 (0.13 0.25)** ***0.18 (0.00 0.38)*** **0.64 (0.39 0.83)**	0.12 (0.08 0.18) *0.11 (−0.03 0.34)*	0.01 (−0.02 0.06) *0.15 (−0.06 0.38)*
BG	0.62 (0.40 0.74)	−0.17 (−0.33 0.08)	0.26 (0.04 0.42)	0.61 (0.37 0.76)	**0.19 (0.14 0.27)** ***0.12 (0.00 0.38)*** **0.69 (0.42 0.84)**	0.02 (−0.02 0.07) *0.17 (−0.05 0.40)*
Cerebellum	0.46 (0.22 0.66)	0.07 (−0.18 0.35)	0.07 (−0.17 0.32)	0.40 (0.17 0.62)	0.33 (0.10 0.56)	**0.21 (0.15 0.29)** ***0.40 (0.04 0.67)*** **0.39 (0.11 0.76)**

Additive genetic effects are given below the diagonal, and environmental effects above the diagonal. The correlations for shared environment are given in italics, below the calculations for the unique environment. The values on the diagonal (in boldface) represent parameter estimates for e^2, c^2, and a^2.

Table 5
Parameter estimates for the best-fit factor model (2-0-2 IPM)

	Common factors				Structure-specific factors			Heritability estimates		
	A1	A2	E1	E2	As	Cs	Es	a^2	c^2	e^2
Cerebrum	0.85*	0.22‡	0.13*	0.29*	0.33‡	0.02	0.14	0.88	0.00	0.12
	(0.76 0.95)	(0.07 0.35)	(0.06 0.21)	(0.21 0.37)	(0.23 0.42)	(−0.48 0.52)	(0.01 0.30)	(0.77 0.91)	(0.00 0.13)	(0.09 0.17)
LV	0.05	0.57*	−0.17‡	0.27*	0.00	0.53	0.54	0.32	0.28	0.39
	(−0.09 0.19)	(0.29 0.84)	(−0.31 −0.03)	(0.14 0.41)	(−0.93 0.93)	(0.29 0.78)	(0.46 0.62)	(0.09 0.68)	(0.00 0.48)	(0.29 0.53)
CC	0.28*	0.06	0.24*	0.06	0.83*	0.26	0.33	0.75	0.06	0.17
	(0.16 0.40)	(−0.11 0.24)	(0.15 0.33)	(−0.02 0.14)	(0.57 0.95)	(−0.61 1)	(0.28 0.38)	(0.40 0.88)	(0.00 0.14)	(0.12 0.24)
Thalamus	0.85*	0.01§	0.40*	0.00§	0.00	0.30	0.17	0.72	0.09	0.19
	(0.76 0.95)		(0.32 0.49)		(−91 0.92)	(0.22 0.37)	(0.07 0.28)	(0.64 0.85)	(0.00 0.14)	(0.14 0.26)
BG	0.84*	−0.17‡	0.31*	−0.01	0.28	0.00	0.31	0.81	0.00	0.19
	(0.74 0.94)	(−0.36 −0.05)	(0.22 0.40)	(−0.09 0.07)	(0.13 0.43)	(−0.37 0.36)	(0.01 0.25)	(0.70 0.86)	(0.00 0.08)	(0.14 0.26)
Cerebellum	0.64*	0.14‡	0.02	0.31*	0.33	0.49	0.34	0.55	0.24	0.21
	(0.53 0.75)	(0.004 0.34)	(−0.08 0.12)	(0.20 0.42)	(−0.01 0.66)	(0.27 0.70)	(0.01 0.26)	(0.36 0.81)	(0.00 0.40)	(0.16 0.29)

A1 and A2 represent common genetic factors, while E1 and E2 are environmental sources unique to individuals, but shared between brain regions. Shared environmental common factors were not statistically significant. Values represent factor loadings, with 95% confidence intervals given in brackets. Factor loadings for structure-specific factors also are given, as are proportional variance components estimates under this model, for each structure in the analysis.

*$p<0.001$; ‡$p<0.05$; §fixed to make factors orthogonal.

Table 6
Genetic and environmental correlations between the cerebrum and other neuroanatomic structures, after segmenting cerebral tissue into gray and white matter

	Additive genetic		Unique environment	
	Gray	White	Gray	White
Cerebral gray	1.00	0.84 (0.65 0.99)	1.00	−0.04 (−0.24 0.17)
Cerebral white	0.84 (0.65 0.99)	1.00	−0.04 (−0.24 0.17)	1.00
LV	0.11 (−0.42 0.65)	0.18 (−0.32 0.72)	0.19 (−0.01 0.37)	0.14 (−0.05 0.33)
CC	0.09 (−0.21 0.39)	0.49 (0.25 0.69)	0.16 (−0.06 0.36)	0.43 (0.25 0.59)
Thalamus	0.88 (0.69 0.99)	0.96 (0.82 1)	0.25 (0.05 0.44)	0.38 (0.20 0.54)
BG	0.77 (0.60 0.91)	0.80 (0.67 0.94)	0.24 (0.03 0.43)	0.16 (−0.05 0.36)
Cerebellum	0.73 (0.44 0.99)	0.88 (0.56 1)	0.57 (0.41 0.69)	0.22 (0.03 0.41)

95% confidence intervals are given in parentheses.

significantly worse than a Cholesky decomposition. However, the 2-2-2 CPM was rejected relative to either the full Cholesky (χ^2_{30}=175.26; p<0.0001; AIC=115.26) or the 2-2-2 IPM (χ^2_{18}=167.21; p<0.0001; AIC=131.21). A stepwise removal of latent factors indicated that the 2-0-2 IPM was once again the best fit model (versus Cholesky: χ^2_{24}=19.3; p=0.6814; AIC=−26.66, versus 2-2-2 IPM: χ^2_{18}=11.2; p 0.4199; AIC=−10.72). However, the patterns of genetic and environmental associations differed substantially when examining residual variance after adjusting for TBV (Table 8). In general, the structures shared less variance with each other, though one common factor indicated that the thalamus and the basal ganglia shared a substantial proportion of their genetic variance, and a second genetic factor influenced both the cerebral compartment and the corpus callosum. Two common individual-specific environmental factors also emerged; one influencing thalamus and the subcortical compartment in an opposite direction to cerebrum and lateral ventricles, and one whose effects influenced cerebrum and cerebellum in opposite directions.

Discussion

One of the fundamental questions in neurogenetics is how our relatively simple genetic programming combines with environmental exposure to produce variation in human brain volumes. Our data suggest that not only do genes play the predominant role in generating the observed volumetric diversity, but that most of the genetic variance is determined by genes that are shared between the major gross neural subdivisions. Concordant with previous univariate studies, the contribution of the shared environment to variance was negligible, while the individual-specific environment had smaller but statistically significant factors common to multiple regions; an environmental factor influencing ROIs beneath the cortical surface (corpus callosum, thalamus, and basal ganglia), and a non-subcortical factor (cerebrum, lateral ventricles, and cerebellum) were identified. Though both genetic and non-genetic effects are critical for explaining neuroanatomic covariance, these data additionally suggest that, at this level of spatial resolution, genes and environment exert their influences on brain variation largely independently of one another.

Such a strong role of genes on the correlations between brain volumes was not unexpected given prior multivariate twin studies. One study methodologically similar to the present one, performed by Barré et al., examined relationships between height, intracranial volume (ICV), total gray matter, total white matter, and lateral ventricular volumes in 54 MZ and 58 DZ adult twin pairs and 34 sibs of DZ pairs via variance component analyses (Baaré et al., 2001). They found remarkably similar estimates of genetic (0.68) and unique environmental (0.04) correlations between gray and white matter, and no statistically significant evidence of genetic correlations between the lateral ventricles and other regions of interest. Nevertheless, the two studies do differ in several aspects, most notably in that the present study includes several neuroanatomic regions of interest while the study by Barré et al. focused on a few global cerebral measures and correlations between these measures and height and ICV. A similar approach was taken in an earlier study by Posthuma et al. which used a trivariate Cholesky decomposition of height, intracranial space, and cerebellar volume in an extended twin design (Posthuma et al., 2000) of 111 twin

Table 7
Genetic and environmental correlations derived after regressing on total brain volume

	Cerebrum	LV	CC	Thalamus	BG	Cerebellum
Cerebrum	1	**0.17 (−0.02 0.36)**	**0.15 (−0.06 0.34)**	**−0.41 (−0.56 −0.22)**	**−0.41 (−0.57 −0.21)**	**−0.16 (−0.35 0.05)**
LV	0.13 (−0.87 0.59)	1	**−0.09 (−0.28 0.12)**	**−0.36 (−0.52 −0.19)**	**−0.33 (−0.49 −0.15)**	**0.20 (0.00 0.38)**
CC	0.34 (0.01 0.82)	0.12 (−0.61 0.68)	1	**0.33 (0.14 0.50)**	**0.22 (0.01 0.41)**	**−0.12 (−0.32 0.09)**
Thalamus	0.34 (−0.16 1)	−0.59 (−0.99 0.32)	0.64 (0.00 0.99)	1	**0.59 (0.44 0.71)**	**−0.27 (−0.44 −0.07)**
BG	0.02 (−0.19 0.80)	−0.88 (−1 −0.34)	0.26 (−0.10 0.64)	0.72 (0.21 1)	1	**−0.10 (−0.29 0.11)**
Cerebellum	−0.09 (−0.96 1)	0.12 (−1 0.85)	−0.23 (−1 0.39)	−0.25 (−0.99 0.82)	−0.03 (−0.90 1)	1

Genetic correlations are given below the diagonal, and unique environmental correlations above the diagonal.

Table 8
Parameter estimates for the best fit model (2-0-2 IPM) after adjusting for total brain volume

	Common factors				Structure-specific factors			Heritability estimates		
	A1	A2	E1	E2	As	Cs	Es	a^2	c^2	e^2
Cerebrum	0.00	0.48	−0.39*	0.40*	0.68‡	0.00	0.01	0.68 (0.35 0.77)	0.00 (0.00 0.30)	0.32 (0.22 0.44)
LV	0.37	0.10	−0.23*	−0.14‡	0.13	0.66	0.57	0.17 (0.06 0.66)	0.43 (0.00 0.55)	0.40 (0.30 0.52)
CC	0.17	0.50	0.08	0.18*	0.60	0.44	0.35	0.65 (0.34 0.88)	0.19 (0.00 0.49)	0.16 (0.11 0.22)
Thalamus	0.52	0.28	0.50*	0.16‡	0.27	0.47	0.30	0.42 (0.23 0.71)	0.22 (0.00 0.38)	0.36 (0.27 0.48)
BG	0.79	−0.03	0.41*	0.06§	0.00	0.00	0.44	0.64 (0.49 0.74)	0.00 (0.00 0.09)	0.36 (0.26 0.50)
Cerebellum	0.05	0.04§	−0.06	−0.23*	0.50	0.69‡	0.46	0.24 (0.00 0.70)	0.49 (0.05 0.74)	0.27 (0.20 0.37)

*$p<0.001$; ‡$p<0.05$; §fixed to make factors orthogonal.

pairs and 34 sibs. They estimate cerebellar heritability of 0.88 with significant sex effects on mean cerebellar volume, with a relatively high genetic correlation to the ICV (0.57) and a low genetic correlation to height (0.25). Though this study represents an important contribution to methodological design and advancement of the use of volumetric data as a novel endophenotype, its focus is not on relationships between brain regions but rather on relationships between brain volumes and non-neural phenotypes.

To date, only two other studies, to our knowledge, have employed genetically informative data to describe multivariate neuroanatomic relationships. A principle components analysis by Pennington et al. on a modest sample of 34 MZ and 32 DZ late teen or young adult twin pairs parcellated the brain into 7 cortical gray compartments and 6 noncortical structures (white matter, basal ganglia, brain stem, hippocampus, cerebellum, and the central gray nuclei including the thalamus) found that two factors could account for 64% of the total phenotypic variance. While cerebral structures loaded primarily on the first factor, all other structures loaded on the second (except central gray, which loaded equally on both). Both factors were significantly more correlated in MZ than in DZ pairs, suggesting a strong genetic component to each. This approach differs substantially from the present study, not only in its use of principal components analyses rather than factor analyses, but also because it generated factors prior to decomposing variance. By contrast, we determined factor structure and variance components simultaneously using maximum likelihood. The study by Pennington et al. also has been criticized since greater than 70% of both MZ and DZ samples had dyslexia, though it is unclear how large of an effect this difference would have on a global multivariate analysis.

Despite the differences in study design, the findings between the two studies are largely complementary. Both find two strong genetic factors influencing inter-structural covariance. The factor loading pattern of the Pennington study does differ in that noncortical structures are not particularly correlated with cortical structures. This discrepancy may be owed in part to the use of ICV as a covariate in the Pennington study. After regressing out the effects of total brain volume, we did observe a genetic factor that was primarily cerebral (total cerebral volume and corpus callosum), with a second genetic factor that loaded on non-cerebral structures (with thalamus loading on both). However, the cerebellar measure in the present study had no genetic covariance with other structures after adjusting for brain volume, while in the Pennington study the cerebellum had a factor loading of 0.71 on the "noncortical" factor. Though the exact cause for the discrepancy is unclear, it could be due to differences in statistical methodology, as principle components analyses include structure-specific variance within its factors, while the factor analytic approach explicitly defines this variance as independent of common factors. Differences in cerebellar quantification also may play a role.

The final extant multivariate twin study by Wright et al. (2002) parcellated the brain into regions with extremely high spatial resolution. Ninety-two (primarily cerebral) gray matter ROIs were automatically defined, roughly according to Brodmann's areas. Global effects were accounted for by adjusting for total gray volumes. Genetic correlations for each ROI pair were first calculated via a series of bivariate factor analyses, and then principle components analyses were applied to the resultant correlation matrix. This study identified two putative supra-regional principle components under genetic control. Specifically, a frontoparietal limbic/paralimbic factor and a factor related to audition (lateral temporal cortex, insula, occipitofrontal, and other frontal regions) were found; factor loadings, however, were quite low (<|0.25|). These findings would suggest that genes are involved in generating functional relationships between distant brain regions. Though extremely provocative, Wright et al.'s study is limited by low power, due to small sample size (10 MZ and 10 same sex DZ pairs) and issues of multiple testing.

The process of neurogenesis is extraordinarily complex. Though neurovolumetric changes are observed throughout childhood (Giedd et al., 1996; Gogtay et al., 2004; Sowell et al., 1999a, b, 2004), the majority of brain formation occurs *in utero* and most of the genes involved in neurodevelopment are also expressed at this time (Rakic and Lombroso, 1998; Rubenstein et al., 1999; Rubenstein and Rakic, 1999). In animal models, a multitude of genes responsible for brain patterning have now been identified, whose products include transcription factors, morphogens, and apoptotic factors (Rubenstein and Rakic, 1999). The initial discovery of the *Hox* family of transcription factors and their segmental patterns of expression in the hindbrain have argued strongly for the neuromeric models of brain organization (Lumsden and Krumlauf, 1996; Mcginnis and Krumlauf, 1992; Puelles, 2001); more recent studies on the forebrain have suggested that although its development is more plastic and cell lineages appear less restricted, the prosencephalon also follows segmental (i.e., prosomeric) patterning based on expression of homeotic and related genes (Anderson et al., 1999; Puelles, 2001; Rubenstein and Rakic, 1999). Though mutations in neurodevelopmental genes have been shown to produce severe pathological states in humans (Clark, 2004), the genetic and environmental agents responsible for typical human variation are still unknown.

Theoretically, genetic associations between neuroanatomic structures could arise via numerous putative mechanisms; several general models can be considered while interpreting the present

data. First, brain volumes may be related genetically via ubiquitous gene products involved in basic cellular metabolism, cell growth, differentiation, or other global processes expressed throughout neuroectodermal derivatives (Rakic, 1995). For example, functional variation in housekeeping genes or cell cycle regulators might be expected to produce genetic correlations between all brain regions that express them (and perhaps other tissues), if they produce downstream effects on volumetric measures via changes in cell proliferation or survival. Second, correlations in brain volumes may represent vestigial relationships generated prenatally between structures with shared ontogenetic origins. Region-specific expression of transcription factors during neuroembryonic patterning would be one example of gene products producing regional correlations during embryogenesis. In this case, one would expect stronger genetic relationships among structures whose development diverged more recently (e.g., thalamic and hypothalamic volumes to be correlated via their shared diencephalic origin). Third, functional interrelationships between structures may generate volumetric correlations via morphological changes associated with increased connectivity. This hypothesis is essentially a generalization of the Protocortex model, which states that neocortical development is determined by extrinsic influences, such as effects of thalamic innervation (O'Leary, 1989; Schlaggar and O'Leary, 1991). Thus, one might expect structures in the visual processing network, such as V1 and the lateral geniculate nucleus, to be structurally correlated despite being potentially unrelated spatially or ontogenetically. Finally, genetic correlations may result from shared supra-regional gene expression triggered postnatally, in the present data from birth to the age of scan acquisition, approximately mid-childhood.

The present data indicate that much of the variability in brain volumes is caused by genes shared between all tissue compartments. This finding is concordant with evolutionary genetic models of brain development which hypothesize global, genetically mediated differences in cell division as the driving force behind interspecies differences in total brain volume (Finlay and Darlington, 1995) as well as with the radial unit hypothesis of neocortical expansion proposed by Rakic (1995). Comparative neuroanatomic analyses of multiple mammalian species have shown that total brain volume is highly correlated with regional volumes, irrespective of region (including neocortex, striatum, thalamus, and cerebellum), and accounts for the vast majority (>96%) of the observed volumetric variance in all regions measured except for the olfactory bulb (Darlington et al., 1999; Finlay and Darlington, 1995). Such strong correlations are thought to reflect a generalized adaption to specific selective pressures; although it is more expensive, in terms of energy, to expand the computational resources of the entire brain when only specific functions are needed, the molecular adjustments required are far fewer than those required to completely repattern gross neural architecture.

In contrast, we found little evidence of genetic factors mediating region-specific neurodevelopment. The most notable ontogenetic "oddball" in the present study was the cerebellum. Developmentally, the cerebellum diverges from the other regions soon after neural tube formation; while cerebrum, corpus callosum, and subcortical structures all are derived from the embryonic prosencephalon, cerebellar tissue is primarily derived from the rombencephalon (Kandel and Jessl, 2000). However, differences in genetic correlations between the cerebellum and other structures were not particularly striking, either before or after removing the effects of TBV. Similarly, we did not detect weaker genetic associations between the thalamus when compared to the telencephalic cerebral volumes or the predominantly telencephalic basal ganglia (Fishell, 1997; Kandel and Jessl, 2000; Puelles, 2001). Though genetically mediated regional brain patterning certainly plays a major and undisputed role in mammalian neurodevelopment, our data would suggest that it plays a surprisingly minor role, at least at our level of volumetric measurement, in the generation of structure-specific *variation* within the typical human population. Functional relationships, for example, may be more important for defining volumetric correlations between the structures measured as basal ganglia, thalamus, and neocortex all are tightly linked functionally.

Though the unique environment had a relatively minor effect on the volumes of the structures measured, our relatively large sample allowed us to describe its role on the correlations between structures with high precision. We found that structures in spatial proximity were significantly and positively correlated via individual-specific environmental factors shared between multiple anatomic regions. In other words, the environment tends to influence nearby structures similarly. The principle exception was that correlations between subcortical nuclei and the lateral ventricles were significantly negatively correlated. Given that atrophy of either the basal ganglia or the thalamus can be associated with increased lateral ventricular volume in several diseases (Gaser et al., 2004; Harris et al., 1999), an antagonistic effect between ventricles and subcortical nuclei was not unexpected. However, as our calculations represent environmental effects in typically developing children, these findings suggest that the correlation is not always pathological. Structural modeling identified two statistically significant putative environmental factors mediating the environmental correlations, one representing subcortical structures and one representing the cerebrum and cerebellum. It is possible that common environmental effects reflect stochastic processes of major effect occurring early in development, or smaller, more continuous processes whose effects are additive.

Despite the wealth of information obtained from this study, certain limitations must be considered. Fundamental to its complex design involving intricate multistep techniques, this study inherits all of the limitations and assumptions of its component pieces, namely studies of twins, volumetric MRI, and structural equation modeling. The twin design is often criticized for its reliance on the equal environment assumption (EEA), which states that, on average, MZ and DZ twin pairs do not differ *relative to the phenotypes of interest*. It is now widely believed that much of the concerns regarding the EEA are overstated at best (Evans et al., 2002); regardless, it is unlikely that general violations of the EEA would substantially impact regional brain volumes (Hulshoff Pol et al., 2002). Secondly, the nature of our predominantly Caucasian, pediatric sample may limit generalizations to other populations. Aging, in particular, could reduce the strength of genetic factors on explaining neurovolumetric variance. Twin studies on geriatric populations, however, have shown that heritability for brain volumes remains high even into the seventh decade of life (Carmelli et al., 2002a,b; Pfefferbaum et al., 2000, 2004), and it is thus unlikely that patterns of neuroanatomic covariance change dramatically over the human lifespan. Thirdly, it is possible that a proportion of the large genetic covariance observed between structures is owed to genes responsible for general body size, rather than brain-specific genetic factors. Though the present study could

not examine the contribution of body size on brain volume, Barré et al. have shown that the genetic correlations between height and total gray or white matter are low (0.19 and 0.16, respectively), suggesting that most of the observed genetic correlations between neuroanatomic structures cannot be explained by body size alone (Baaré et al., 2001).

Finally, the limitations of our phenotypic measurements and image processing methodology may influence the results. For example, our volumetric measures may be disproportionately sensitive to the proliferative and apoptotic components of neurodevelopment. The use of morphometrics, such as deformation-based morphometry (Ashburner et al., 1998) rather than volumetric approaches might be more able to detect regionalized topological similarities that reflect common embryologic origins.

Acknowledgments

J.E.S. was supported by an NIH NRSA training fellowship, MH-20030; M.C.N. was supported by NIH grants MH-65322 and DA-18673.

References

Achenbach, T.M., Ruffle, T.M., 2000. The Child Behavior Checklist and related forms for assessing behavioral/emotional problems and competencies. Pediatr. Rev. 21 (8), 265–271.

Akaike, H., 1987. Factor analysis and AIC. Psychometrika 52, 317–332.

Anderson, S., Mione, M., Yun, K., Rubenstein, J.L.R., 1999. Differential origins of neocortical projection and local circuit neurons: role of Dlx genes in neocortical interneuronogenesis. Cereb. Cortex 9, 646–654.

Ashburner, J., Hutton, C., Frackowiak, R., Johnsrude, I., Price, C., Friston, K., 1998. Identifying global anatomical differences: deformation-based morphometry. Hum. Brain Mapp. 6, 348–357.

Baaré, W.F., Hulshoff Pol, H.E., Boomsma, D.I., Posthuma, D., De Geus, E.J., Schnack, H.G., Van Haren, N.E., van Oel, C.J., Kahn, R.S., 2001. Quantitative genetic modeling of variation in human brain morphology. Cereb. Cortex 11, 816–824.

Bartley, A.J., Jones, D.W., Weinberger, D.R., 1997. Genetic variability of human brain size and cortical gyral patterns. Brain 120 (Pt 2), 257–269.

Biondi, A., Nogueira, H., Dormont, D., Duyme, M., Hasboun, D., Zouaoui, A., Chantome, M., Marsault, C., 1998. Are the brains of monozygotic twins similar? A three-dimensional MR study. AJNR Am. J. Neuroradiol. 19, 1361–1367.

Carmelli, D., Reed, T., DeCarli, C., 2002a. A bivariate genetic analysis of cerebral white matter hyperintensities and cognitive performance in elderly male twins. Neurobiol. Aging 23, 413–420.

Carmelli, D., Swan, G.E., DeCarli, C., Reed, T., 2002b. Quantitative genetic modeling of regional brain volumes and cognitive performance in older male twins. Biol. Psychol. 61, 139–155.

Clark, G.D., 2004. The classification of cortical dysplasias through molecular genetics. Brain Dev. 26, 351–362.

Collins, D.L., Neelin, P., Peters, T.M., Evans, A.C., 1994. Automatic 3D intersubject registration of MR volumetric data in standardized Talairach space. J. Comput. Assist. Tomogr. 18, 192–205.

Collins, D.L., Holmes, C.J., Peters, T.M., Evans, A.C., 1995. Automatic 3-D model-based neuroanatomical segmentation. Hum. Brain Mapp. 190–208.

Crawford, C.B., DeFries, J.C., 1978. Factor analysis of genetic and environmental correlation matrices. Multivar. Behav. Res. 13, 297–318.

Darlington, R.B., Dunlop, S.A., Finlay, B.L., 1999. Neural development in metatherian and eutherian mammals: variation and constraint. J. Comp. Neurol. 411, 359–368.

Edwards, A.W.F., 1972. Likelihood. Cambridge, London.

Evans, D.M., Gillespie, N.A., Martin, N.G., 2002. Biometrical genetics. Biol. Psychol. 61, 33–51.

Falconer, D.S., Mackay, T.F.C., 1996. Introduction to Quantitative Genetics. Longman, Essex.

Faraone, S.V., Seidman, L.J., Kremen, W.S., Kennedy, D., Makris, N., Caviness, V.S., Goldstein, J., Tsuang, M.T., 2003. Structural brain abnormalities among relatives of patients with schizophrenia: implications for linkage studies. Schizophr. Res. 60, 125–140.

Finlay, B.L., Darlington, R.B., 1995. Linked regularities in the development and evolution of mammalian brains. Science 268, 1578–1584.

Fishell, G., 1997. Regionalization in the mammalian telencephalon. Curr. Opin. Neurobiol. 7, 62–69.

Gaser, C., Nenadic, I., Buchsbaum, B.R., Hazlett, E.A., Buchsbaum, M.S., 2004. Ventricular enlargement in schizophrenia related to volume reduction of the thalamus, striatum, and superior temporal cortex. Am. J. Psychiatry 161, 154–156.

Giedd, J.N., Snell, J.W., Lange, N., Rajapakse, J.C., Casey, B.J., Kozuch, P.L., Vaituzis, A.C., Vauss, Y.C., Hamburger, S.D., Kaysen, D., Rapoport, J.L., 1996. Quantitative magnetic resonance imaging of human brain development: ages 4–18. Cereb. Cortex 6, 551–560.

Gogtay, N., Giedd, J.N., Lusk, L., Hayashi, K.M., Greenstein, D., Vaituzis, A.C., Nugent, T.F., Herman, D.H., Clasen, L.S., Toga, A.W., Rapoport, J.L., Thompson, P.M., 2004. Dynamic mapping of human cortical development during childhood through early adulthood. Proc. Natl. Acad. Sci. U. S. A. 101, 8174–8179.

Harris, G.J., Codori, A.M., Lewis, R.F., Schmidt, E., Bedi, A., Brandt, J., 1999. Reduced basal ganglia blood flow and volume in pre-symptomatic, gene-tested persons at-risk for Huntington's disease. Brain 122, 1667–1678.

Herbert, M.R., Ziegler, D.A., Deutsch, C.K., O'Brien, L.M., Lange, N., Bakardjiev, A., Hodgson, J., Adrien, K.T., Steele, S., Makris, N., Kennedy, D., Harris, G.J., Caviness, V.S., 2003. Dissociations of cerebral cortex, subcortical and cerebral white matter volumes in autistic boys. Brain 126, 1182–1192.

Hulshoff Pol, H.E., Posthuma, D., Baare, W.F., De Geus, E.J., Schnack, H.G., Van Haren, N.E., van Oel, C.J., Kahn, R.S., Boomsma, D.I., 2002. Twin-singleton differences in brain structure using structural equation modelling. Brain 125, 384–390.

Kandel, E., Jessl, 2000. Principles of Neural Science. McGraw Hill.

Kendler, K.S., Heath, A.C., Martin, N.G., Eaves, L.J., 1987. Symptoms of anxiety and symptoms of depression-same genes, different environments. Arch. Gen. Psychiatry 44, 451–457.

Loehlin, J.C., 1996. The Cholesky approach: a cautionary note. Behav. Genet. 26, 65–69.

Lumsden, A., Krumlauf, R., 1996. Patterning the vertebrate neuraxis. Science 274, 1109–1115.

Mcardle, J.J., Goldsmith, H.H., 1990. Alternative common factor models for multivariate biometric analyses. Behav. Genet. 20, 569–608.

Mcginnis, W., Krumlauf, R., 1992. Homeobox genes and axial patterning. Cell 68, 283–302.

Neale, M.C., Cardon, L.R., 1992. Methodology for Genetic Studies of Twins and Families. Kluwer Academic, Dordrecht, the Netherlands.

Neale, M.C., Miller, M.B., 1997. The use of likelihood-based confidence intervals in genetic models. Behav. Genet. 27, 113–120.

Neale, M.C., Boker, S.M., Xie, G., Maes, H.H., 1999. Mx: Statistical Modeling. Department of Psychiatry, Medical College of Virginia. Virginia Commonwealth University, Richmond, VA.

O'Leary, D.D.M., 1989. Do cortical areas emerge from a protocortex. Trends Neurosci. 12, 400–406.

Orr, H.A., 1887. Contribution to the embryology of the lizard. J. Morphol. 1, 311–372.

Pennington, B.F., Filipek, P.A., Lefly, D., Chhabildas, N., Kennedy, D.N., Simon, J.H., Filley, C.M., Galaburda, A., DeFries, J.C., 2000. A twin MRI study of size variations in human brain. J. Cogn. Neurosci. 12, 223–232.

Pfefferbaum, A., Sullivan, E.V., Swan, G.E., Carmelli, D., 2000. Brain structure in men remains highly heritable in the seventh and eighth decades of life. Neurobiol. Aging 21, 63–74.

Pfefferbaum, A., Sullivan, E.V., Carmelli, D., 2004. Morphological changes in aging brain structures are differentially affected by time-linked

environmental influences despite strong genetic stability. Neurobiol. Aging 25, 175–183.
Posthuma, D., De Geus, E.J., Neale, M.C., Hulshoff Pol, H.E., Baare, W.E.C., Kahn, R.S., Boomsma, D., 2000. Multivariate genetic analysis of brain structure in an extended twin design. Behav. Genet. 30, 311–319.
Puelles, L., 2001. Brain segmentation and forebrain development in amniotes. Brain Res. Bull. 55, 695–710.
Rakic, P., 1995. A small step for the cell, a giant leap for mankind—A hypothesis of neocortical expansion during evolution. Trends Neurosci. 18, 383–388.
Rakic, P., Lombroso, P.J., 1998. Development of the cerebral cortex: I. Forming the cortical structure. J. Am. Acad. Child Adolesc. Psych. 37, 116–117.
Ramnani, N., Behrens, T.E.J., Penny, W., Matthews, P.M., 2004. New approaches for exploring anatomical and functional connectivity in the human brain. Biol. Psychiatry 56, 613–619.
Reveley, A.M., Reveley, M.A., Chitkara, B., Clifford, C., 1984. The genetic-basis of cerebral ventricular volume. Psychiatry Res. 13, 261–266.
Rubenstein, J.L.R., Rakic, P., 1999. Genetic control of cortical development. Cereb. Cortex 9, 521–523.
Rubenstein, J.L.R., Anderson, S., Shi, L.M., Miyashita-Lin, E., Bulfone, A., Hevner, R., 1999. Genetic control of cortical regionalization and connectivity. Cereb. Cortex 9, 524–532.
SAS Institute, 2000. SAS/STAT User's Guide. SAS institute, Cary, NC.
Scamvougeras, A., Kigar, D.L., Jones, D., Weinberger, D.R., Witelson, S.F., 2003. Size of the human corpus callosum is genetically determined: an MRI study in mono and dizygotic twins. Neurosci. Lett. 338, 91–94.
Schlaggar, B.L., O'Leary, D.D.M., 1991. Potential of visual-cortex to develop an array of functional units unique to somatosensory cortex. Science 252, 1556–1560.
Schmitz, S., Cherny, S.S., Fulker, D.W., 1998. Increase in power through multivariate analyses. Behav. Genet. 28, 357–363.
Sled, J.G., Zijdenbos, A.P., Evans, A.C., 1998. A nonparametric method for automatic correction of intensity nonuniformity in MRI data. IEEE Trans. Med. Imag. 17, 87–97.
Sowell, E.R., Thompson, P.M., Holmes, C.J., Batth, R., Jernigan, T.L., Toga, A.W., 1999a. Localizing age-related changes in brain structure between childhood and adolescence using statistical parametric mapping. NeuroImage 9, 587–597.
Sowell, E.R., Thompson, P.M., Holmes, C.J., Jernigan, T.L., Toga, A.W., 1999b. In vivo evidence for post-adolescent brain maturation in frontal and striatal regions. Nat. Neurosci. 2, 859–861.
Sowell, E.R., Thompson, P.M., Leonard, C.M., Welcome, S.E., Kan, E., Toga, A.W., 2004. Longitudinal mapping of cortical thickness and brain growth in normal children. J. Neurosci. 24, 8223–8231.
Steinmetz, H., Herzog, A., Schlaug, G., Huang, Y., Jancke, L., 1995. Brain (A) symmetry in monozygotic twins. Cereb. Cortex 5, 296–300.
Tien, A.Y., Eaton, W.W., Schlaepfer, T.E., McGilchrist, I.K., Menon, R., Powers, R., Aylward, E., Barta, P., Strauss, M.E., Pearlson, G.D., 1996. Exploratory factor analysis of MRI brain structure measures in schizophrenia. Schizophr. Res. 19, 93–101.
Tramo, M.J., Loftus, W.C., Stukel, T.A., Green, R.L., Weaver, J.B., Gazzaniga, M.S., 1998. Brain size, head size, and intelligence quotient in monozygotic twins. Neurology 50, 1246–1252.
von Baer, K.E., 1828. Uber die Enwicklungsgeschichte der Thiere, Beobachtung und Reflexion. Borntrager, Konigsberg.
White, T., Andreasen, N.C., Nopoulos, P., 2002. Brain volumes and surface morphology in monozygotic twins. Cereb. Cortex 12, 486–493.
Wright, I.C., Sharma, T., Ellison, Z.R., McGuire, P.K., Friston, K.J., Brammer, M.J., Murray, R.M., Bullmore, E.T., 1999. Supra-regional brain systems and the neuropathology of schizophrenia. Cereb. Cortex 9, 366–378.
Wright, I.C., Sham, P., Murray, R.M., Weinberger, D.R., Bullmore, E.T., 2002. Genetic contributions to regional variability in human brain structure: methods and preliminary results. NeuroImage 17, 256–271.
Zijdenbos, A., Forghani, R., Evans, A.C., 2002. Automatic "pipeline" analysis of 3-D MRI data for clinical trials: application to multiple sclerosis. IEEE Trans. Med. Imag. 21, 1280–1291.